URSI AP-RASC, Sydney, Australia, 17 – 22 August 2025

Using COTS antennas for Multifaceted Array Structure with Geometric Analysis

Yanyan Zhang*, Rodney Vaughan
Sierra Wireless Laboratory, Simon Fraser University, BC, Canada, www.sfu.ca/sierra-wireless-lab

Abstract

A method is presented for solving the geometric design of multifaceted array antenna structure where arrays on all the visible facets contribute to the total array. The projected area of the multifaceted structure to the far-field is the primary metric, and configurations are sought that minimize its variation across the field-of-view, which is most challenging when it covers the hemispherical set of directions. General cases are analyzed and in particular the method can be applied for different application scenarios that have different height limitation requirements. A motivation is to be able to reduce production costs by using mass-produced commercial of-the-shelf (COTS) antennas for the arrays on each facet.

1 Background and Introduction

The field-of-view (FoV) is the angular range where an antenna can direct its beam to achieve some performance metric, usually gain, often accompanied by a polarization purity requirement. For wall- and ceiling-mounted antennas, and terrestrial-to-satellite links, the largest FoV and most challenging to realize, is the entire hemisphere. The most economical manufacturing approach is a single planar array, which also has the advantage of a minimum height profile. But conventional planar arrays have compromised gain in directions approaching their horizon. This paper concerns the design of multi-faceted arrays which solve the gain to the horizon at the cost of a more complicated structure, and in particular, a higher profile structure.

A hemispherical FoV is sought in indoor applications such as LANs [1] and surveillance [2]; and outdoor applications, classically terrestrial antennas for low-earth-orbit (LEO) satellite communications [3]. It has been noted, e.g., [4], that multifaceted phased arrays can enable new services from the booming business of small satellites in LEOs.

The design of multifacted arrays continues to be a topic of research, owing to the complexity of the design choices complicating an optimization formulation. Generally, a full-wave numerical solution for a practical-sized antenna, is not possible because the overall structure is too big to solve with commercial software. This puts solver-based optimization out of the question currently. The first open publications on design were in the 1960s when, for a hemispherical FoV, Knittel [5] sought an optimal number of facets and Kmetzo [6] sought an optimal facet angle for pyramidal structures. Later, Corey [7] sought an optimal facet angle with an element packing geometry for scan limits approaching a hemispheric FoV, and Khalifa and Vaughan [8] [9] formulated a minimax method for pyramid and pyramidal frustum structures. Previous work has used one facet at a time to achieve the FoV, i.e., the signal combining from the arrays was tacitly considered as switched or selection combining. Here, the arrays on all the visible facets are assumed to be simultaneously combined, specifically equal-gain combined. Using maximum-ratio (the optimum linear combination for resulting maximum signal-to-noise ratio) or even optimum-combining (for maximum signal-to-noise-plus-interference) of the array signals is fertile ground for new research. The details of the elements (number, layout and orientation) of the planar arrays on each facet are not addressed here, it is simply assumed that the gain and a geometric projection of a facet are related, in order to derive a multifaceted structure ready for population by elements. This paper supplements submitted work [10] by including a general height constraint, a major design parameter for many applications.

2 Description of Structure

2.1 Modeling

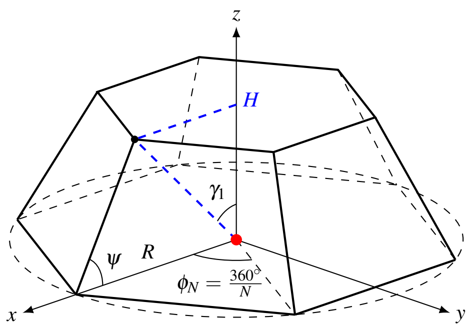

Figure 1. A pyramidal frusta with $N = 6$ showing the modeling terms.

A pyramidal frustra is shown in Figure 1. The modeling terms are: the number of side facets, N, defining the facet angle $\phi_N = 2\pi/N$; the radius of a circle enclosing the footprint, R, which is normalized by the wavelength, λ; the zenith angle to the vertices of the top facet, γ_1; the angle between the corner of the side facets and the mounting plane, ψ. The height of the pyramidal frusta (or just a pyramid) is

$$H = \frac{R\sin(\psi)\cos(\gamma_1)}{\sin\left(\frac{\pi}{2}+\gamma_1-\psi\right)}. \tag{1}$$

Figure 2 shows some special cases for, e.g., $N = 6$: (a) for $\psi = 0°$, a planar structure consisting of N triangles. (b) for $\gamma_1 = 90°$, - another planar structure but consisting of a single facet with zero-height side facets. (c) for $\psi = 90°$, a prism structure. (d) for $\gamma_1 = 0°$, a pyramid. The limiting

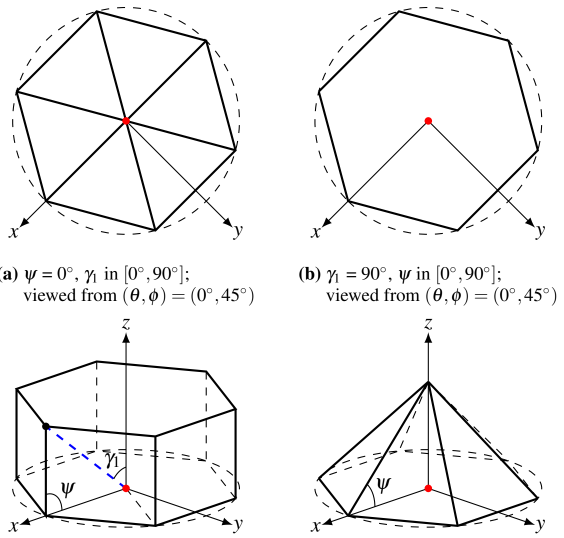

(a) $\psi = 0°$, γ_1 in $[0°, 90°]$; viewed from $(\theta,\phi) = (0°, 45°)$

(b) $\gamma_1 = 90°$, ψ in $[0°, 90°]$; viewed from $(\theta,\phi) = (0°, 45°)$

(c) $\psi = 90°$, γ_1 in $(0°, 90°)$; viewed from $(\theta,\phi) = (70°, 45°)$

(d) $\gamma_1 = 0°$, ψ in $(0°, 90°)$; viewed from $(\theta,\phi) = (70°, 45°)$

Figure 2. Limiting cases of the multifaceted model, case $N = 6$

cases of a planar aperture are taken as benchmarks for presenting the results below. This formulation allows a script to be developed that can quickly undertake brute force optimization, viz., stepping through (γ_1, ψ, N) and finding the total projected area of the structure from the far-field viewing angles (θ, ϕ).

2.2 Variation of the Visible Aperture

A major assumption is now made - that the total projected area to the far field is proportional to the effective aperture of the multi-array antenna, i.e., can be considered as proportional to the directive gain. A decibel unit (as often used for gain) is used here for the range of the gain within the FoV,

$$Variation\ (\text{dB}) = 10\log_{10}\left(\frac{\text{Total Projected Area}_{max}}{\text{Total Projected Area}_{min}}\right). \tag{2}$$

For the benchmark planar case, the maximum projected area is at the array broadside ($\theta = 0°$), and the minimum projected area is at the horizon, $\theta = 90°$. For non-zero-height structures, via increasing N, the maximum projected area will approach the structure's footprint, πR^2, so

$$0 \leq Total\ Projected\ Area^{(\text{Planar Structure})} < \pi R^2. \tag{3}$$

For the planar configurations, the *Variation* range approaches infinity ($\frac{Area_{max}}{0}$); and for $N \to \infty$, i.e., a hemispherical structure, we have

$$Variation^{(\text{Hemispherical})} \to 10\log_{10}\left(\frac{\pi R^2}{\pi R^2/2}\right) = 3\ \text{dB}. \tag{4}$$

3 Constrained Structure

3.1 Height Constraint

Using the *Variation (dB)* term of (2) to viualize a first-cut of the performance from the multifaceted structure model, the dependence on N, γ_1 and ψ is illustrated in Figure 3. Here, stacked heat maps indicate how the *Variation* changes for a given number of facets. The structures with the desired minimum *Variation*, are almost the same for all N. This is because the minimum corresponds to a tall multifaceted pyramid, but this an unlikely design choice because of the intrusive form factor of the excess height.

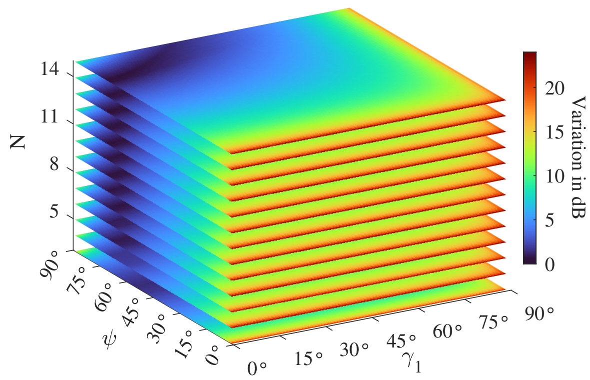

Figure 3. Stacked heat map view of the range of the projected area in dB for $N \in [3-15]$ plotted on the z-axis against ψ and γ_1

In practical applications where the height of the antenna array is constrained, the approaches for limiting the height include [10]:

- setting the areas of all facets to be similar so that the distribution of the antenna placement will be easier;
- setting a constant height which is likely to be a design specification, which may vary by application;
- setting a height limitation with constraining profile (including fixed height), such as being within an inscribing hemisphere.

To study the impact of the height, the height-to-footprint radius ratio is used (again as a dB unit for convenience) :

$$H/R\ (\text{dB}) = 10\log_{10}\left(\frac{Structure\ \mathbf{H}eight}{Footprint\ \mathbf{R}adius}\right). \tag{5}$$

Figure 4 is H/R contours against γ_1 and ψ. $H/R > 0$ dB means that the structure is taller than the enclosing hemispherical with radius of the footprint.

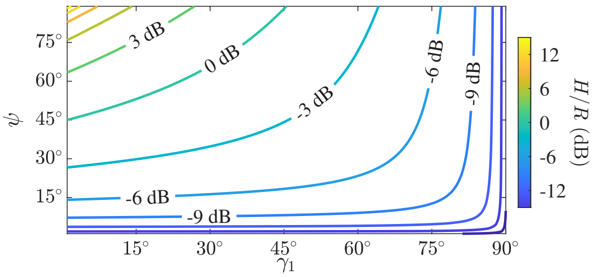

Figure 4. Contour of H/R against (γ_1, ψ). After [10]

3.2 Height Constraint Example

For the sake of demonstration, the height follows from the inscribing hemisphere illustrated in Figure 5 (a) with $\psi = \gamma_1/2 + 45°$. The *Variation* and H/R against γ_1 for

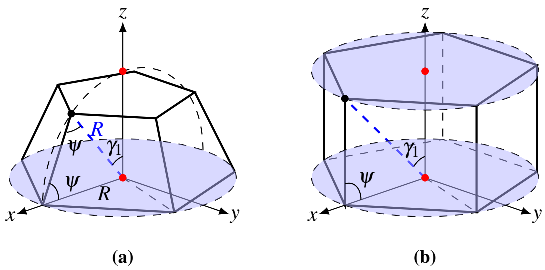

Figure 5. Illustration of a height limitation profile: A multifaceted pyramidal frustum enclosed by a) hemisphere; b) cylinder.

these designs is presented in Figure 6 with parameter N, for pyramidal frusta and pyramids ($\gamma_1 = 0°$). From the figure, the $N = 3$ cases have the minimum *Variation*, and in fact after $N = 4$, the *Variation* behavior is not sensitive to N for a given $\gamma_1(\psi)$. There is low sensitivity for $\gamma_1 \in (15°, 45°)$. This plot does not indicate the difference of the area of the top facet and a side facet, a practical design parameter considered below.

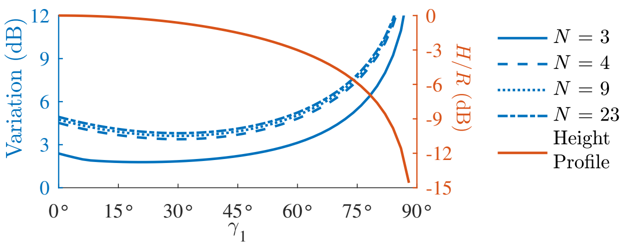

Figure 6. *Variation* against γ_1 with the hemispheric height constraint, with N as a parameter. The Height line follows the locus of equation (6).

4 Summary of Results

Three general design cases are presented, supplementing the results of [10]. These are classified as:

- **"without Limit"**: structures without any height limitation but not including the open cases where the height is infinite;
- **"with Height Limit"**: structures with height limitation, the region of interest is $H/R \leq 0$ dB in Figure 4, i.e., analysis is omitted outside this region. The structure is capped by the cylinder as shown in Figure 5 (b).
- **"with Height and View Limit"**: structures with height limitation ($H/R \leq 0$ dB) and partial hemispherical coverage given by the FoV of $\theta \in [0°, 75°]$.

The results are in Figure 7. The top graph shows the structures with the minimum *Variation* against $N \in [3, 15]$. The middle graph is the H/R, and the bottom plot is the ratio of the areas of the top facet to a side facet.

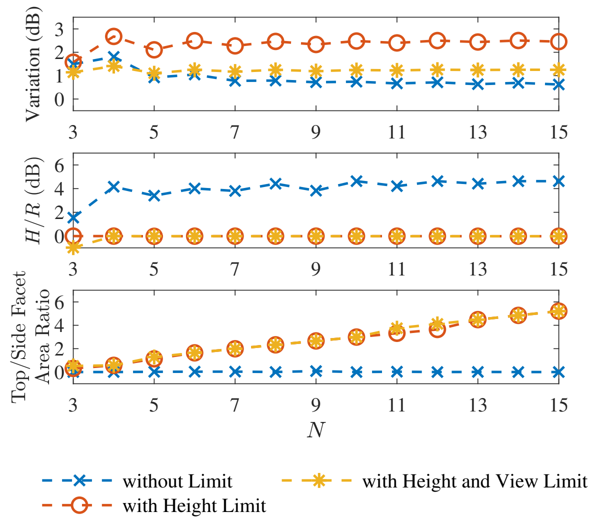

Figure 7. Comparison between structures for full and partial hemispherical coverage (FoV $\theta \leq 75°$), with constrained height.

The structures having the lowest *Variation* are considered optimal in the sense of having the most consistent gain across the FoV. The cases with no height constraint (marked with a cross) are the best, with their *Variation* heading to just below 1dB, and the structure is a tall pyramidal frustum as indicated in the middle plot. For $N = 3$, the H/R of the minimum *Variation* structure is 1.5 dB ($\approx$ 1.42 times) greater than the footprint radius, which is similar to the PAVE PAWS structure [11].

The constrained-height pyramidal frustum structure (marked with circles) has its *Variation* just below 3dB (so just lower than that of a hemispheric structure), whereas for the case of constrained height and partial coverage (marked with stars), it is around 1dB. The minimum *Variation* has hit diminishing returns after $N = 7$ for all the cases.

However, from the bottom plot of Figure 7, as N increases, the relative areas of the top and side facets are changing, showing that $N = 5$ is optimal, based on the area of the top facet being almost the same as the side facet (a ratio of 1.1:1), which facilitates similar-sized arrays all facets. Having compatible areas for all facets fosters being able to use similar COTS arrays antennas on all the facets. The $N = 5$ structure is also optimal for the partial coverage example (FoV of $0^o \leq \theta \leq 75^o$).

5 Review of Assumptions

The basic assumption in an optics-based approach such as used here, is that a total projected area of a multifaceted array offers an approximation to the total effective area, i.e., the available gain. The variation of this total projected area therefore relates to the gain changes over the FoV. As noted in [10], this basic assumption will hold if: i) the facet sizes are electrically big enough to house sufficient array elements to allow a reasonably linear relation between the number of elements and their array gain; ii) the scan loss of each facet-born array is not too large, i.e., the required scan angles for the array on each facet are modest; and iii) the signal combination of the multiple arrays is economically feasible. The element details and multiple-array signal combining are not addressed here. In skipping these, an important performance issue that is not addressed here is the polarization purity which is normally (eg. in a planar array only) an element-only issue, but for multifacted arrays it is complicated by needing to combine the different arrays on different facets which will have different polarization distributions depending on the element orientations.

6 Summary and Conclusion

The design of multifaceted arrays has been an ongoing subject of research papers due to the complexity of formulating the design choices. An ideal approach would be to use commercial solvers to undertake the design optimization because this would include the many complicating factors such as diffraction contributions from the facet edges, mutual coupling, particularly the orientation of the elements on each facet, and the associated gain and polarization perturbations. But such an approach is not currently feasible owing to the large electrical size of a reasonable-sized multifacteted array. The simplest approach is to begin with the optical approximation (total projected area proportional to gain) to get a first-cut basic geometric configuration, which is the subject of this paper. This establishes robust (in the sense that the formulation is well-defined) geometric designs, i.e., those where small changes in the structure should not significantly impact the overall performance. Whereas previous work has considered a single facet at-a-time coverage, the method presented here is for the case where arrays on all the visible facets to a given view angle are simultaneously signal-combined. Once the basic basic structure is established (for example from the method of this paper), then the element layout for the arrays can be tackled. This is for future research.

References

[1] L.-M. Zhang, X. Ding, and B.-Z. Wang, "A Low-Cost Beam Steering Antenna for Indoor Wireless Communication," IEEE Transactions on Antennas and Propagation, vol. 70, no. 9, pp. 8548–8553, 2022.

[2] A. Andaya Lestari, L. Simbolon, R. O. Bura, O. D. Winarko, and B. K. Pradekso, "UWB Wire-Bowtie Array for FM-PCL Passive Radar," IEEE Transactions on Antennas and Propagation, vol. 70, no. 9, pp. 7999–8007, 2022.

[3] M. Geissler, F. Woetzel, M. BÃűttcher, S. Korthoff, A. Lauer, M. Eube, and M. Wleklinski, "Design and test of an L-band phased array for maritime satcom," in Proceedings of the 5th European Conference on Antennas and Propagation (EUCAP), 2011, pp. 2871–2875.

[4] G. He, X. Gao, L. Sun, and R. Zhang, "A Review of Multibeam Phased Array Antennas as LEO Satellite Constellation Ground Station," IEEE Access, vol. 9, pp. 147 142–147 154, 2021.

[5] G. Knittel, "Choosing the number of faces of a phased-array antenna for hemisphere scan coverage," IEEE Transactions on Antennas and Propagation, vol. 13, no. 6, pp. 878–882, 1965.

[6] J. Kmetzo, "An analytical approach to the coverage of a hemisphere by n planar phased arrays," IEEE Transactions on Antennas and Propagation, vol. 15, no. 3, pp. 367–371, 1967.

[7] L. Corey, "A graphical technique for determining optimal array antenna geometry," IEEE Transactions on Antennas and Propagation, vol. 33, no. 7, pp. 719–726, 1985.

[8] I. Khalifa and R. Vaughan, "Geometric Design of Pyramidal Antenna Arrays for Hemispherical Scan Coverage," IEEE Transactions on Antennas and Propagation, vol. 55, no. 2, pp. 468–471, 2007.

[9] I. Khalifa and R. G. Vaughan, "Geometric Design and Comparison of Multifaceted Antenna Arrays for Hemispherical Coverage," IEEE Transactions on Antennas and Propagation, vol. 57, no. 9, pp. 2608–2614, 2009.

[10] Y. Zhang and R. Vaughan, "Geometric analysis of signal-combined multifaceted array structures," 2025, unpublished manuscript.

[11] Wikipedia contributors, "PAVE PAWS — Wikipedia, the free encyclopedia," 2024, [Online; accessed 12-May-2024]. [Online]. Available: https://en.wikipedia.org/w/index.php?title=PAVE_PAWS&oldid=1218735495